Controllable Synthesis of Na, K-based Titanium Oxide Nanoribbons as Functional Electrode for Supercapacitor and Separation of Aqueous Ions

Hao Zhang,[a,#,] Fang Zhang,[b,#,]* Aiyang Li,[a,c] Bin Zhao,[d] Danni Li,[b] Yifei Liu,[a,b] Yang Yang,[a]*

*Fangzhou Li,[b] Rui Liu,[e] Yuquan Wei[e,]**

a: Technical Centre for Soil, Agriculture and Rural Ecology and Environment, Ministry of Ecology and Environment, Beijing 100012, PR China.
b: School of Environment and state Key Joint Laboratory of Environment Simulation and Pollution Control, School of Environment, Tsinghua University, Beijing 100084, PR China.
c: Environmental Standard Institute, Ministry of Ecology and Environment, Beijing 100012, PR China
d: Institute of Eco-environmental and Soil Sciences, Guangdong Academy of Sciences, Guangzhou 510650, PR China
e. Beijing Key Laboratory of Biodiversity and Organic Farming, College of Resources and Environmental Sciences, China Agricultural University, 100193 Beijing, PR China

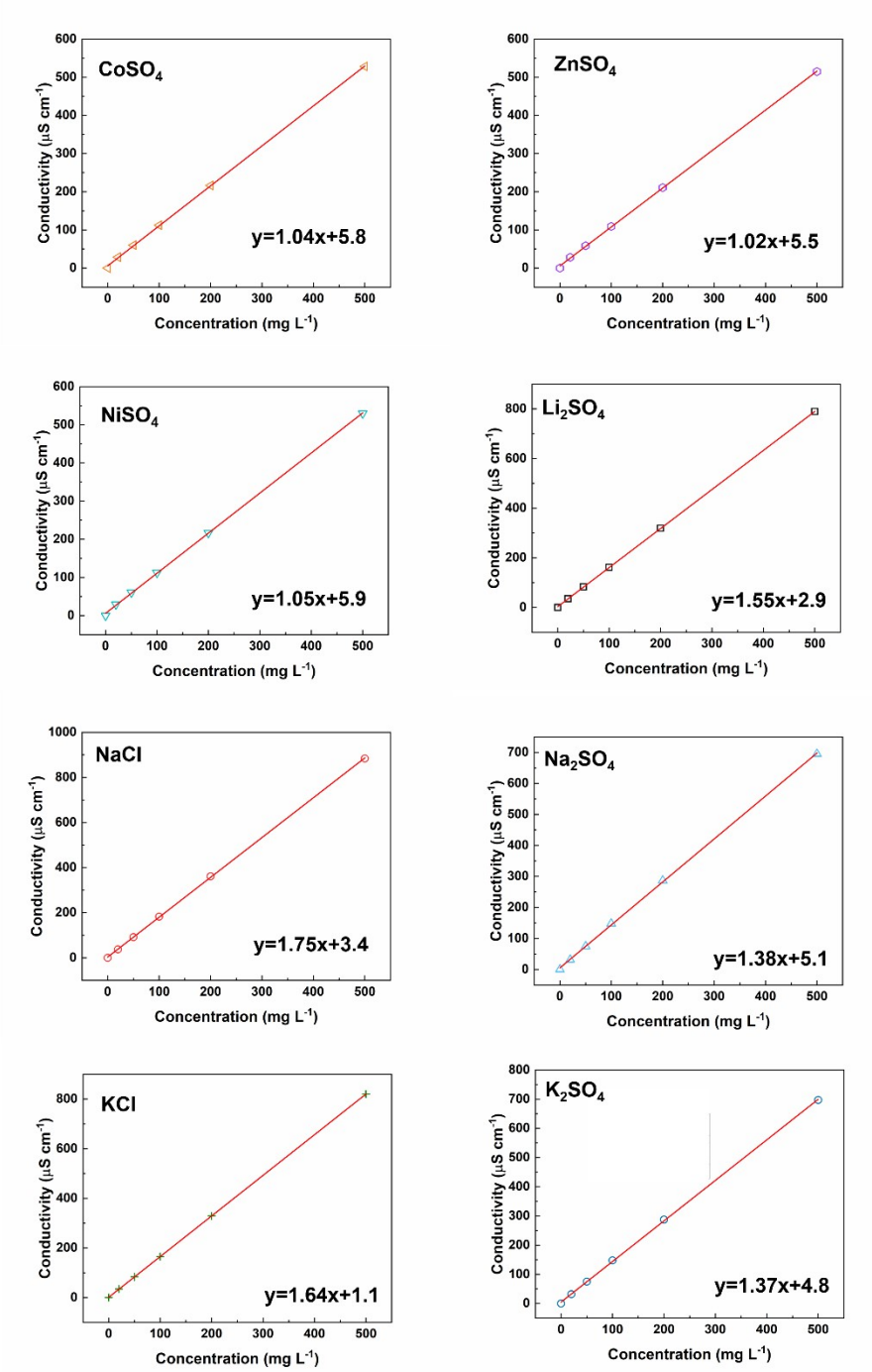

Figure S1. Calibration curve of conductivity to eight saline solution concentration.

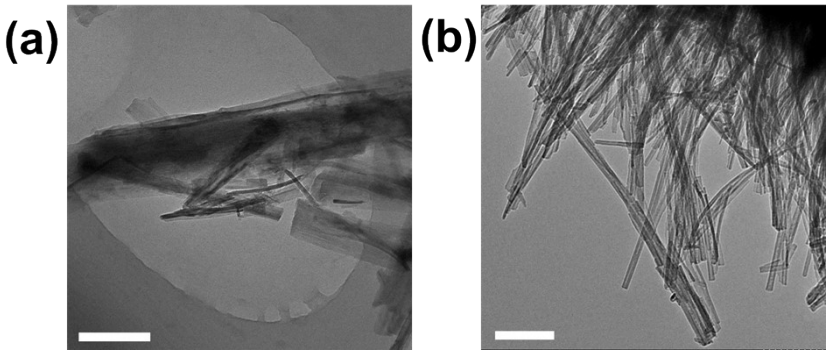

Figure S2. Morphological characterization of MTO materials: (a) KTO; (b)NTO whisker TEM images.

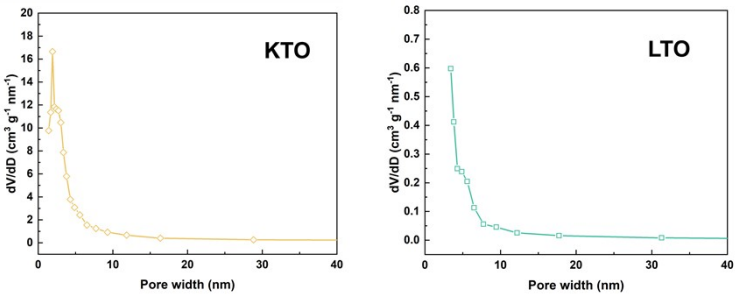

Figure S3. Pore width distribution of LTO and KTO materials.

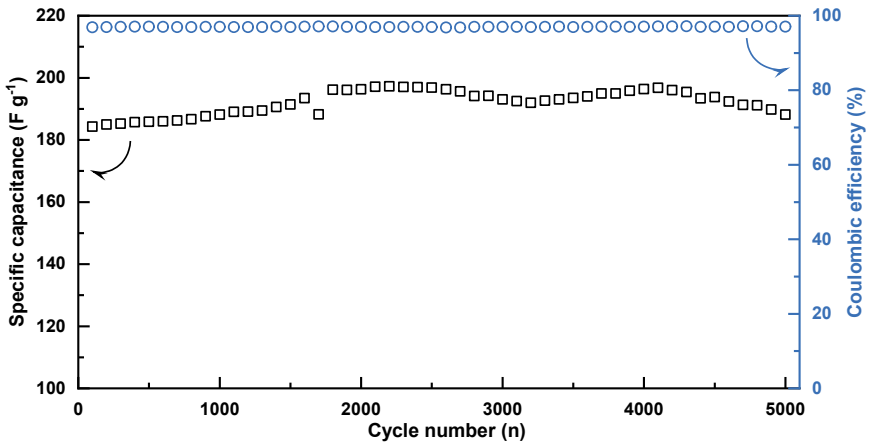

Figure S4. Long-term charge/discharge cycles KTO electrode.

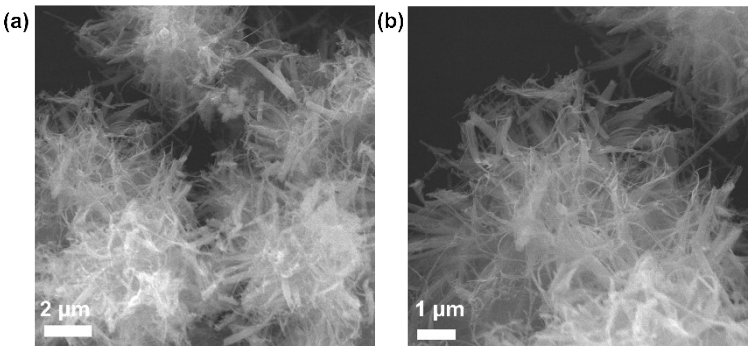

Figure S5. Morphology of KTO after cycling of SEM images.

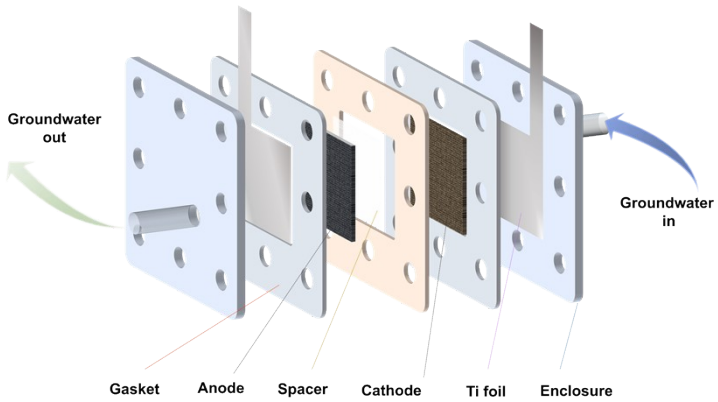

Figure S6. Schematic illustration of asymmetric CDI device.

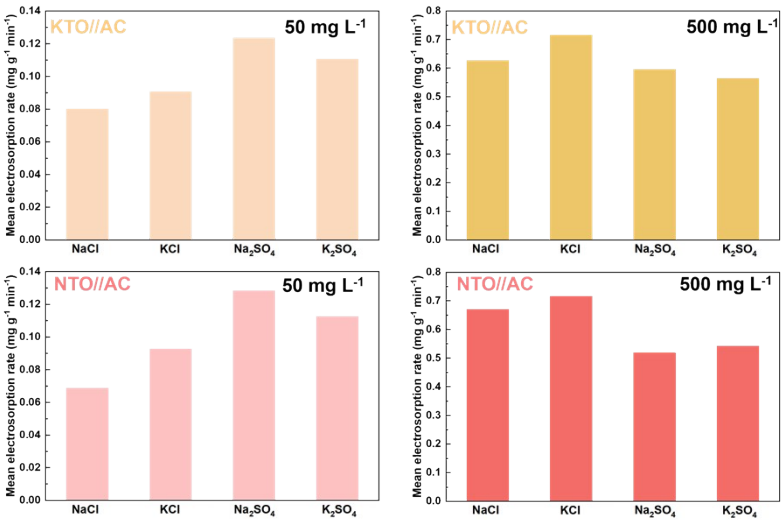

Figure S7. Electrosorption/desorption rate performance of NTO//AC and KTO//AC CDI device in various saline solutions with different concentration.

Table S1 Values of specific capacitance depending on galvanostatic discharge curves of different electrodes.

Current density A g^{-1}		1	2	5	10	20
Specific capacitance F g^{-1}	LTO	172.5	155.3	137.1	119.2	93.6
	NTO	182.3	166.1	145.9	128.0	99.8
	KTO	196.6	184.2	159.1	137.0	108.3

Table S2 Comparison of NTO and KTO with reported works for the electrochemical performance

Materials	Specific capacitance ($F\ g^{-1}$)	Capability rate (%)	Electrolyte	Ref.
SWCNTs/TiO_2 nanocomposite	144	91	PVA/H_2SO_4	1
Mn_3O_4 nanorod	136.5	36.6	Na_2SO_4	2
C-TiO_2	214	67.3	Na_2SO_4	3
TiO_2@BAC	402.5	21.1	KOH	4
TiO_2-CNT	345.7	43.1	H_2SO_4	5
Sn-doped TiO_2 NTAs	329	-	H_2SO_4	6
$Na_2Ti_3O_7$/SWCNTs	576.01		KOH	7
TiO_2/CDC	173.2	60	Na_2SO_4	8
NTO	182.3	54.7	KOH	This work
KTO	196.6	55.1	KOH	This work

Table S3 Comparison of different desalination materials with reported works for the desalination performance

Electrode	Saline solution	Capacity	Work voltage	Ref.
ACC:ZnO	NaCl，100 mg L^{-1}	8.5 mg g^{-1}	1.2 V	11
ZnO/AC	NaCl，500 mg L^{-1}	9.4 mg g^{-1}	1.2 V	12
Gr/SnO_2	NaCl，30 mg L^{-1}	1.49 mg g^{-1}	1.4 V	13
Fe_3O_4/rGO	$CaCO_3$，35 mg L^{-1}	4.3 mg g^{-1}	1.5 V	14
Zr/ACC	NaCl，5.8 mg L^{-1}	2.05 mg g^{-1}	1.0 V	15
MoS_2	NaCl，400 mg L^{-1}	8.81 mg g^{-1}	1.2 V	16
TiO_2/CNTs	NaCl，500 mg L^{-1}	4.3 mg g^{-1}	1.2 V	17
TiO_2NTs/HCF/CF	Na_2SO_4，55 mg L^{-1}	1.69 mg g^{-1}	1.6 V	18
Ti-C	NaCl，50 mg L^{-1}	7.11 mg g^{-1}	1.4 V	19
ZnO/ACC	NaCl，1660 mg L^{-1}	5.72 mg g^{-1}	1.5 V	20
rGO@MnO_2	NaCl，50 mg L^{-1}	3.50 mg g^{-1}	1.2 V	21
Carbon aerogel/MnO_2	NaCl，1461 mg L^{-1}	6.4 mg g^{-1}	1.5 V	22
RuO_2(20)-AC	NaCl，292.2 mg L^{-1}	11.3 mg g^{-1}	1.2 V	23
MO/ACF	$Cd(NO_3)_2$，18 mg L^{-1}	10.5 mg g^{-1}	1.5 V	24
ACC-TiO_2	NaCl，1000 mg L^{-1}	5.3 mg g^{-1}	1.5 V	12
TiO_2/rGO	NaCl，500 mg L^{-1}	25.0 mg g^{-1}	1.2 V	9
Ti-C	NaCl，50 mg L^{-1}	9.61 mg g^{-1}	1.4 V	19
MnO_2/CNT–CS	NaCl，877 mg L^{-1}	10.07 mg g^{-1}	1.6 V	25
Mn@C-400	NaCl，25 mg L^{-1}	5.4 mg g^{-1}	1.2 V	26
CNTs/rGO	NaCl，~500 mg L^{-1}	1.4 mg g^{-1}	1.2 V	10
Ti-ACC	NaCl，250 mg L^{-1}	2.05 mg g^{-1}	1.0 V	27
KTO//AC	KCl，500 mg L^{-1}	7.35 mg g^{-1}	1.6 V	This work

References

[1] M. Lal, R. Badam, N. Matsumi, S. Ramaprabhu, Hydrothermal synthesis of single-walled carbon nanotubes/TiO_2 for quasi-solid-state composite-type symmetric hybrid supercapacitors, J. Energ. Storage, 2021, 40, 102794.

[2] H. Zhang, D. Liu, Y. Wei, A. Li, B. Liu, Y. Yuan, H. Zhang, G. Li and F. Zhang, Fabrication of A 1D Mn_3O_4 Nano-Rod Electrode for Aqueous Asymmetric Supercapacitors and Capacitive Deionization, Inorg. Chem. Front., 2019, 6, 355-365.

[3] R. Bortamuly, V. Naresh, M. R. Das, V. K. Kumar, S. Muduli, S. K. Martha, P. Saikia, Titania supported bio-derived activated carbon as an electrode material for high-performance supercapacitors, J. Energ. Storage, 2021, 42, 103144.

[4] A. Ahmed, C. Bathula, R. Soni, H. S. Kim, H. Im, S.-W. Lee, W. K. Kim, S. Gedi, A. Kadam, Nanostructurally engineered TiO_2 embedded Mentha aquatica biowaste derived carbon for supercapacitor applications, Chemosphere, 2022, 289, 133197.

[5] J. Li, J. Ao, C. Zhong, T. Yin, Three-dimensional nanobranched TiO_2-carbon nanotube for high performance supercapacitors, Appl. Surf. Sci. 2021, 563, 150301.

[6] Q. Liu, Y. Yang, Y. Ni, Q. Wang, H. Yu, X. Zhu, Z. Ying, Y. Song, A general approach to the fabrication of Sn-doped TiO_2 nanotube arrays with titanium vacancies for supercapacitors, 2021, 570, 151175.

[7] S.V.P. Vattikuti, K. C. Devarayapalli, N. N. Dang and J. Shim, 1D/1D $Na_2Ti_3O_7$/SWCNTs electrode for split-cell-type asymmetric supercapacitor device, Ceram. Int., 2021, 47, 11602–11610.

[8] W. Zhong, H. Sun, J. Pan, Y. Zhang, X. Yan, Y. Guan, W. Shen, X. Cheng, Hierarchical porous TiO_2/carbide-derived carbon for asymmetric supercapacitor with enhanced electrochemical performance, Mater. Sci. Semicond. Proc. 2021, 127, 105715.

[9] Liu X, Liu H, Mi M, et al. Nitrogen-doped hierarchical porous carbon aerogel for high-performance capacitive deionization [J]. Separation and Purification Technology, 2019, 224:44-50.

[10] Hu N, Meng L, Gao R, et al. A facile route for the large scale fabrication of graphene oxide papers and their mechanical enhancement by cross-linking with glutaraldehyde. Nano-Micro Lett. 2011, 3:215-222.

[11] Myint M, Al-Harthi S H, Dutta J. Brackish water desalination by capacitive deionization using zinc oxide micro/nanostructures grafted on activated carbon cloth electrodes. Desalination, 2014, 344, 236-242.

[12] Liu J, Lu M, Yang J, et al. Capacitive desalination of ZnO/activated carbon asymmetric capacitor and mechanism analysis. Electrochimica Acta, 2015, 151, 312-318.

[13] Tang K, Hong T, You L, et al. Carbon-metal compound composite electrodes for capacitive deionization: synthesis, development and applications. Journal of Materials Chemistry A, 2019, 7(47):26693-26743.

[14] Trinh N T, Chung S, Lee J K, et al. Development of high quality Fe_3O_4/rGO composited electrode for low energy water treatment. Journal of Energy Chemistry, 2016, 25, 354-360.

[15] Ryoo M, Seo G. Improvement in capacitive deionization function of activated carbon cloth by titania modification. Water Research, 2003, 37(7):1527-1534.

[16] Xing F, Li T, Li J, et al. Chemically exfoliated MoS_2 for capacitive deionization of saline water. Nano Energy, 2017, 31:590-595.

[17] Li H, Ma Y, Niu R. Improved capacitive deionization performance by coupling TiO_2 nanoparticles with

carbon nanotubes. Separation and Purification Technology, 2016, 171:93-100.

[18] Wei K, Wang Y, Han W, et al. Fabrication and characterization of TiO_2-NTs based hollow carbon fibers/carbon film composite electrode with NiOx decorated for capacitive application. Journal of Power Sources, 2016, 318:57-65.

[19] Omosebi A, Gao X, Holubowitch N, et al. Anion exchange membrane capacitive deionization cells [J]. Journal of the Electrochemical Society, 2017, 164(9):E242-E247.

[20] Laxman K, Kimoto D, Sahakyan A, et al. Nanoparticulate dielectric overlayer for enhanced electric fields in a capacitive deionization device. ACS Applied Materials & Interfaces, 2018, 10(6):5941-5948.

[21] El-Deen A G, Barakat N, Kim H Y. Graphene wrapped MnO_2-nanostructures as effective and stable electrode materials for capacitive deionization desalination technology. Desalination, 2014, 344:289-298.

[22] Zafra M C, Lavela P, Rasines G, et al. A novel method for metal oxide deposition on carbon aerogels withpotential application in capacitive deionization of saline water. Electrochimica Acta, 2014, 135:208-216.

[23] Ma X, Chen Y, Zhou K, et al. Enhanced desalination performance via mixed capacitive-Faradaic ion storage using RuO_2-activated carbon composite electrodes. Electrochimica Acta, 2019, 295:769-777.

[24] Chen Y, Peng L, Zeng Q, et al. Removal of trace Cd(II) from water with the manganese oxides/ACF composite electrode [J]. Clean Technologies and Environmental Policy, 2015, 17:49-57.

[25] Liu Y, Yu T, Chen Y, et al. Incorporating manganese dioxide in carbon nanotube-chitosan as a pseudocapacitive composite electrode for high-performance desalination. ACS Sustainable Chemistry & Engineering, 2018, 6(3):3196-3205.

[26] Zhao C, Lv X, Li J, et al. Manganese oxide nanoparticles decorated ordered mesoporous carbon electrode for capacitive deionization of brackish water. Journal of the Electrochemical Society, 2017, 164(13):E505-E511.

[27] Ryoo M, Kim J, Seo G. Role of titania incorporated on activated carbon cloth for capacitive deionization of NaCl solution. Journal of Colloid and Interface Science, 2003, 264(215):414-419.